WATER RESOURCES RESEARCH, VOL. 30, NO. 5, PAGES 1287–1297, MAY 1994

Evaluation of hydrologic parameters in a semiarid rangeland using remotely sensed spectral data

M. S. Moran,[1] T. R. Clarke [1] W. P. Kustas,[2] M. Weltz,[3] and S. A. Amer[4]

Abstract. A study was conducted to determine the relation between remotely sensed spectral data and measurements of vegetation-related hydrologic parameters in a semiarid rangeland in southeast Arizona. Throughout the measurement periods, ranging from June to September 1990, eight sites in the U.S. Department of Agriculture's Agricultural Research Service Walnut Gulch experimental watershed were monitored for water and energy fluxes and other meteorological and biological parameters. Corresponding spectral data were acquired with ground-based radiometers, low-altitude aircraft-mounted instruments, and Landsat thematic mapper sensors. Spectral indices were derived from measurements of surface reflectance, based on their response to variations in hydrologic parameters and sensitivity to unrelated variables, such as solar zenith angle and soil differences. A soil-adjusted vegetation index, SAVI (derived from red and NIR reflectance factors), was found to be highly correlated with the temporal changes in vegetation cover and biomass, but less successful in discriminating spatial differences in cover and biomass across the watershed. Significant relations were found between the surface-air temperature ($T_s - T_a$) difference and measurements of soil moisture content, though the shape differed from that previously published for bare soil. The relation between daily evaporation rate and measurements of ($T_s - T_a$) and daily net radiation was similar to that derived previously for irrigated pasture and dryland shortgrass in France but differed from that derived for irrigated wheat. These results emphasized the strengths and limitations of the use of spectral data for estimation of hydrologic characteristics of sparsely vegetated sites and suggested a need for reevaluation of common empirical relations between remotely sensed measurements and surface characteristics for application to rangeland areas.

Introduction

A major objective of hydrology is to better understand and quantify the processes that cause the changes in hydrologic storages and fluxes at local and regional scales. This is necessary to assess the role of the hydrologic cycle in a global context and predict the effects of natural and anthropogenic changes on climate. Toward this goal, numerical hydrological models have been developed to evaluate surface conditions and the energy/water budget and to monitor their long-term evolution [*Shuttleworth and Wallace*, 1985; *Sellers et al.*, 1986]. Most of these approaches require information about initial states (e.g., soil moisture) and knowledge of the spatial and temporal distribution of several surface characteristics (e.g., vegetation cover).

Remotely sensed spectral measurements can provide an indirect means of deriving geophysical quantities required as inputs to hydrological models. Satellite- and ground-based measurements of surface reflectance and temperature have been related to critical model requirements, such as soil moisture [*Idso et al.*, 1975], land cover [*Tucker*, 1979], precipitation [*Rosema*, 1990], and vegetation status [*Jackson*, 1982]. Furthermore, surface temperature and reflectance have been combined with ground-based meteorological data to directly evaluate surface energy fluxes, such as net radiation and evaporation [*Jackson et al.*, 1977]. These relations are generally semiempirical and often site-specific, so they must be reevaluated for application to new geographic regions and different ecosystems. However, once the relationship is obtained and verified, it is possible to obtain integrated values of the hydrologic components at catchment and regional scales using satellite-based sensors.

An ecosystem of particular interest to hydrologists is arid and semiarid rangeland. This ecosystem covers over 40% of the Earth's land surface and is one of the more sensitive land types to climate anomalies and land use practices. A recent experiment conducted at the Walnut Gulch experimental watershed (WGEW) in southeast [*Kustas et al.*, 1991] provided the opportunity to derive relationships between remotely sensed data and basic hydrologic factors for a semiarid rangeland. This report presents an analysis of the variation of surface reflectance and temperature with the hydrologic factors of vegetation cover and biomass, soil moisture, and daily surface evaporation.

[1]U.S. Water Conservation Laboratory, Agricultural Research Service, U.S. Department of Agriculture, Phoenix, Arizona.
[2]Hydrology Laboratory, Agricultural Research Service, U.S. Department of Agriculture, Beltsville, Maryland.
[3]Southwest Watershed Research Center, Agricultural Research Service, U.S. Department of Agriculture, Tucson, Arizona.
[4]Department of Hydrology and Water Resources, University of Arizona, Tucson.

Paper number 93WR03066.
0043-1397/94/93WR-03066$05.00

during each flight to document the ground location of spectral measurements. The flying altitude for the aircraft was a nominal 150 m AGL, resulting in a spatial resolution (a pixel) of approximately 40 m diameter on the surface. The Cessna was flown several times per day along the two parallel transects containing the eight METFLUX stations [*Kustas and Goodrich*, this issue, Figure 4a] starting around 0900 MST each day, except during conditions of significant cloud cover.

The reflectance panel measurements recorded by the ground-based instruments during each flight were used to calculate the aircraft-based reflectance factors of the various ground surfaces. The procedure was to compare the voltages from the two radiometers over a calibrated reflectance panel before and after the flight, calculate a ratio of the aircraft-based to ground-based Exotech voltages, and multiply the ground-based panel readings by this ratio. Knowing the absolute reflectance calibration of the panel, the reflectance factors of the various ground surfaces measured from the aircraft were calculated.

Cloudy conditions during July and August precluded attempts to acquire a Landsat thematic mapper (TM) scene during the monsoon season. However, a clear sky scene was obtained during the dry season (June 5, 1990), and another scene was obtained during the postmonsoon season (September 9, 1990) with partly cloudy sky conditions. The nominal spectral bands of the TM sensor include the visible, NIR, midinfrared, and thermal spectrum (TM1: 0.45–0.52 μm (blue); TM2: 0.53–0.61 μm (green); TM3: 0.62–0.69 μm (red); TM4: 0.78–0.90 μm (NIR); TM5: 1.57–1.78 μm (mid-IR); TM7: 2.10–2.35 μm (mid-IR); and TM6: 10.42–11.66 μm (thermal)).

The spectral reflectance data were converted to spectral "vegetation indices" (VIs) which are more sensitive than individual reflectance factors to vegetation characteristics such as biomass and percent vegetation cover. The normalized difference vegetation index (NDVI) is simply the difference between the NIR and red reflectances (ρ) divided by their sum [*Tucker*, 1979],

$$\mathrm{NDVI} = (\rho_{\mathrm{NIR}} - \rho_{\mathrm{red}})/(\rho_{\mathrm{NIR}} + \rho_{\mathrm{red}}). \quad (2)$$

Though the NDVI facilitates the classification and monitoring of vegetation, it is also sensitive to soil background differences. *Huete* [1988] developed a soil-adjusted vegetation index (SAVI) to account for soil background effects,

$$\mathrm{SAVI} = [(\rho_{\mathrm{NIR}} - \rho_{\mathrm{red}})/(\rho_{\mathrm{NIR}} + \rho_{\mathrm{red}} + L)](1 + L), \quad (3)$$

where L is the soil correction term, suggested by *Huete* [1988] to be 0.5 for optimum results over a wide range of vegetation densities.

Atmospheric Data

To convert Landsat TM digital counts (DC) to values of surface reflectance, atmospheric optical depth was measured on the day of each Landsat overpass, and a radiative transfer code (RTC) was used to compute the relationship between surface reflectance and radiance at the sensor. Measurements of incident solar illumination were made with a solar radiometer over the time period from sunrise to solar noon, and total optical depth of the atmosphere was determined from the slopes of Langley plots [*Slater et al.*, 1987]. Total optical depth was partitioned into Rayleigh, aerosol, and ozone optical depths using the procedure described by *Biggar et al.* [1990]. These values were used as input to the Herman-Browning RTC [*Herman and Browning*, 1965] to provide at-satellite radiance values for several assumed values of surface reflectance, ranging from 0.02 to 0.6. Based on these RTC-derived values and the TM sensor calibration, Landsat TM DCs were converted to surface reflectance factors. This procedure is similar to that described by *Holm et al.* [1989] and *Moran et al.* [1990].

Since radiosonde profiles of atmospheric temperature, water content, and pressure were not available during the Landsat overpasses, retrieval of surface temperatures from the Landsat thermal data (TM6) was achieved by comparing the surface temperature measurements (T_s) at the Kendall target with an average of the corresponding TM6 DCs to compute a DC-to-T_s conversion factor (Table 1).

Table 1. Surface Temperature Measurements During the Landsat TM Overpasses on DOY 156 and 252 and Corresponding Landsat TM6 Digital Counts

DOY	T_{min}	T_{max}	T_{MF5}	$\mathrm{DC}_{\mathrm{MF5}}$	DC/°C
156	43.0	53.6	50.9	198.8	3.907
252	30.4	39.0	35.0	154.7	4.417

T_{min} and T_{max} are the minimum and maximum surface temperatures measured along the north and south flight lines during the Landsat overpasses. T_{MF5} is the surface temperature measured by the yoke-based instruments at the Kendall target. $\mathrm{DC}_{\mathrm{MF5}}$ is the average of Landsat TM6 digital counts corresponding to the Kendall ground target. DC/°C is the ratio of $\mathrm{DC}_{\mathrm{MF5}}$ and T_{MF5} in units of digital count per degree Celsius.

Emissivity

Surface emissivities (ε) ranging from 0.971 at MF1 to 0.985 at MF5 were computed for the METFLUX sites using a technique described by *Humes et al.* [this issue]. Measurements of ε within the spectral wavelength band of the instrument are necessary to convert radiometric surface temperature (T_r) measured with an IRT to absolute (kinetic) surface temperature (T_s) [see *Humes et al.*, this issue]. Based on the narrow range of ε measured at the eight METFLUX sites, it appeared that ε was relatively consistent across the grass/shrub continuum. Consequently, an average ε of 0.98 was assumed for all sites during the monsoon and postmonsoon periods, resulting in less than a 1°C correction in most cases. For the dry season when grasses and forbs were not green, ε was computed as an average of the emissivities of the soil and shrubs weighted by their percent cover at each METFLUX site. This resulted in a dry season emissivity ranging from 0.972 at MF8 to 0.957 at MF4 with an average value of 0.961.

Approach for Estimation of Daily Evaporation From Remotely Sensed Data

An expression relating daily surface evaporation rate (E_d) in units of millimeters per day to $T_s - T_a$ (degrees Celsius) was developed by *Jackson et al.* [1977] based on a simplification of (1),

$$E_d = R_{nd} - G_d - B(T_s - T_a), \quad (4)$$

Table 2. Description of Soils Illustrated in Figure 1

Symbol	Name	Color
BeB	Bernardino gravelly loam, 3–8% slope	brown (7.5YR 4/2) to dark reddish brown (5YR 3/3)
BhB	Bernardino-Hathaway gravelly loam, 3–8% slope	
BhC	Bernardino-Hathaway gravelly loam, 8–15% slope	
Co	Comoro sandy loam	dark brown 7.5YR 4/2) to dark brown (7.5YR 3/2)
HnC	Hathaway-Nickel gravelly loam, 8–15% slope	greyish-brown (10YR 5/2) to dark brown (10YR 3/3)
So	Sonoita sandy loam	yellowish-brown (7.5YR 6/4) to dark yellowish-brown (10YR 4/4)

From *Gelderman* [1970].

appeared to vary less than the NDVI along nonriparian sections of the transect, likely due to its inherent insensitivity to soil background influences.

Solar Zenith Angle

The reflectance measured from vegetated surfaces varies as the angle of the Sun changes due to changes in the proportion of shadows in the scene. The behavior of NIR and red radiance in shadow has been studied by several investigators in order to enhance understanding of the use of VIs [*Jackson et al.*, 1979; *Pinter et al.*, 1983; *Ranson and Daughtry*, 1987; *Singh and Cracknell*, 1985]. Since the NIR transmittance by vegetation is greater than that of the red band, the shadows are "enriched" in the NIR relative to the red. *Ranson and Daughtry* [1987] reported that for low- and medium-density canopies, NDVI increased with increasing solar zenith angles, that is, with increasing proportion of shadow. However, when large amounts of green vegetation were present, NDVI saturated, and the observed dependence was reduced.

For this analysis a subset of the ground-based spectral data was selected for dates between DOY 213 and 222 in which the Sun was either unobstructed or had only light cirrus interference during the measurement period. For this limited time period there was little change in the vegetation cover or biomass, so changes in the VI were attributable largely to other factors. For the Lucky Hills and the north and south facing Kendall targets, the red and NIR reflectance factors were analyzed as a function of the mean solar zenith angle (θ_z) (Figure 2). For all three sites the red reflectance decreased substantially with increasing θ_z. The NIR reflectance decreased to a lesser extent with θ_z for the north facing Kendall and Lucky Hills targets and increased slightly for the south facing Kendall target. As a consequence of the red reflectance's approaching zero, the NDVI increased with θ_z, eventually approaching a maximum value of one. The SAVI showed a similar trend, though the increase was less dramatic than for the NDVI. It was apparent that the effect of θ_z on values of NDVI and SAVI was not only substantial, but also site specific. This makes any attempt to compensate for such effects very difficult.

Results and Discussion

Based on the substantial, site-specific influence of solar zenith angle on surface reflectance and VIs, it was necessary to limit further data analysis to measurements of surface reflectance at low solar zenith angles, corresponding to a measurement time of ≈1030 MST (the approximate time of the Landsat overpass). Five dates were chosen in 1990 and one in 1991 (Table 3) to cover a variety of soil moisture and vegetation density conditions while maintaining relatively cloud-free conditions during the Cessna and Landsat overflights. For each date the ground-based data at Lucky Hills and Kendall were averaged to produce a single estimate of

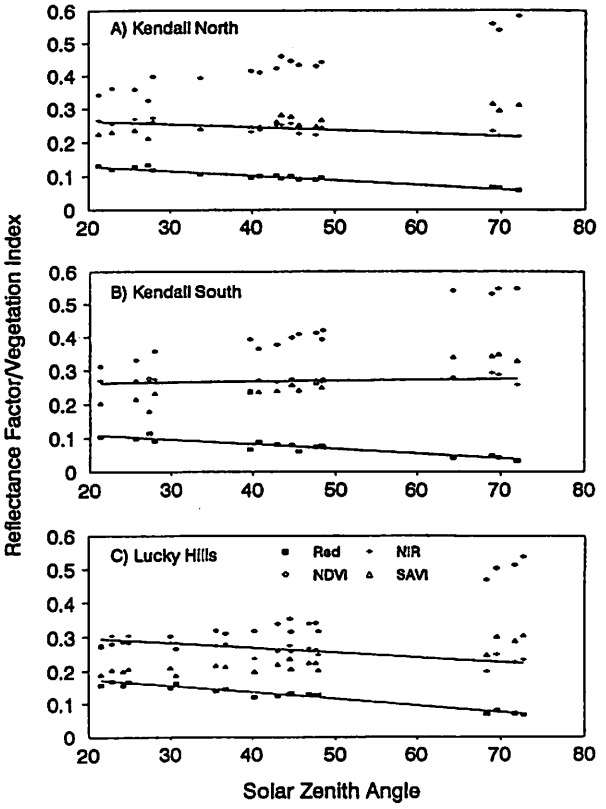

Figure 2. Evaluation of the influence of solar zenith angle differences on surface reflectance factors and vegetation indices using all clear sky ground-based measurements from DOY 213 to 222 at (a) Kendall north facing target, (b) Kendall south facing target, and (c) Lucky Hills. Solid lines represent least squares regression lines fit to the red and NIR reflectance factor data.

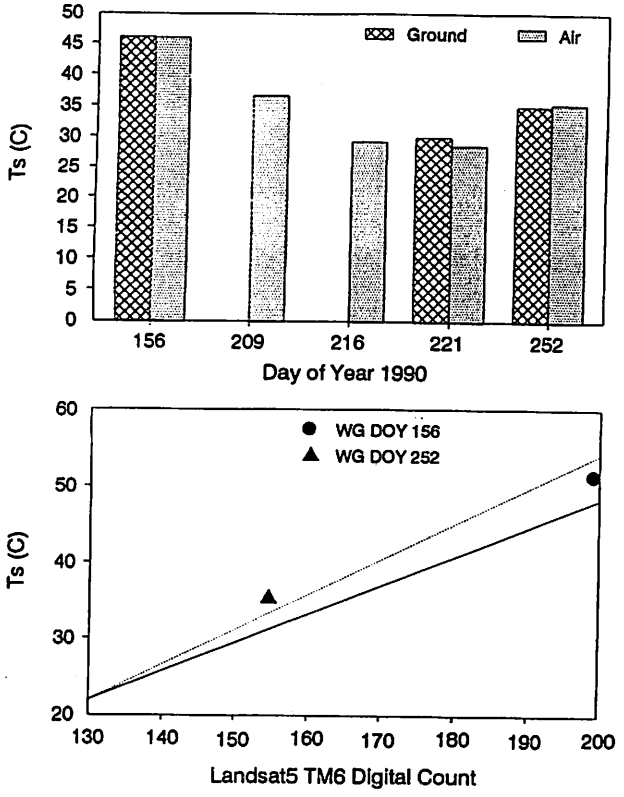

Figure 4. (a) Surface temperature (T_s) measured with ground- and aircraft-based sensors at the Kendall target. (b) Empirical relations between surface temperature (T_s) and Landsat 5 TM6 digital count (DC) for "clear" atmospheric conditions. The dotted line represents the regression equation proposed by *Lathrop and Lillesand* [1986] (equation (10)), and the solid line represents that proposed by *Malaret et al.* [1985] (equation (11)). The solid circle and triangle are the DC-to-T_s conversion factors derived from Kendall data for DOYs 156 and 252.

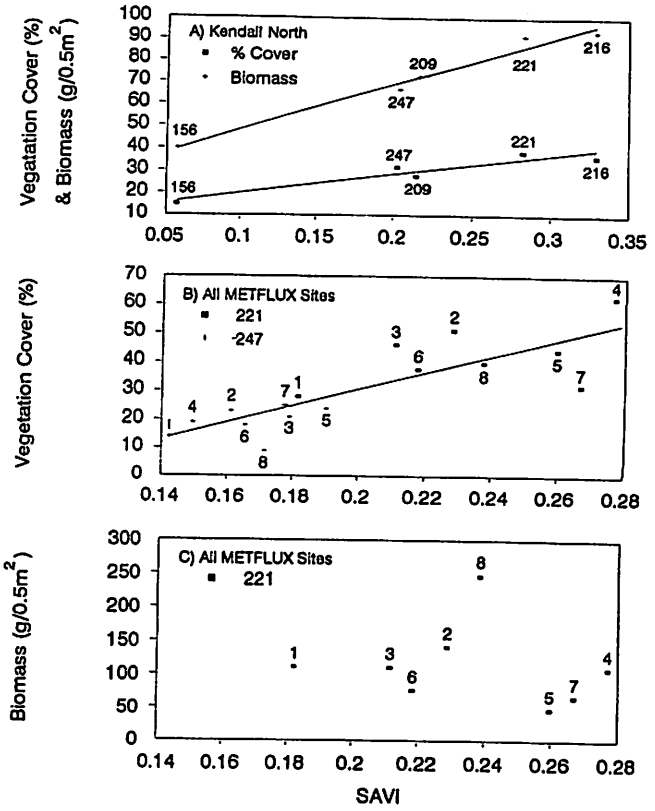

Figure 6. Relation between the soil-adjusted vegetation index (SAVI) measured using airborne sensors and (a) percent vegetation cover and biomass at the Kendall site, (b) percent vegetation cover and (c) biomass at all eight METFLUX sites (labeled 1–8) on DOYs 221 and 247. Solid lines represent the best fit linear regression line; statistics are included as follows for each of three lines illustrated. For Figure 6a, percent cover, $r^2 = 0.98$; $Y = 23.8 + 242.7X$. For Figure 6a, biomass, $r^2 = 0.91$; $Y = 9.6 + 101.4X$. For Figure 6b, percent cover, $r^2 = 0.70$; $Y = 27.5 + 290.3X$.

single day. The variance between values of T_s at the METFLUX sites was greatest on DOY 156 when soil moisture was lowest, and was least on DOY 216, immediately after a rainfall event. This was due to the damping effect of soil moisture on surface temperature variation. On the other hand, SAVI varied significantly with time and space during the monsoon season. For all METFLUX sites, there was a strong correlation between surface temperature and SAVI ($r = 0.93$), implying the sensitivity of both values to similar surface characteristics.

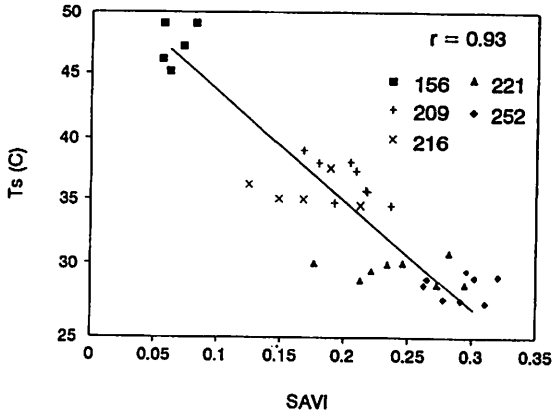

Figure 5. Comparison of surface temperature measurements (T_s) and the soil-adjusted vegetation index (SAVI) for eight METFLUX sites over five measurement dates: DOYs 156, 209, 216, 221, and 252.

Vegetation Cover and Biomass

The relation between SAVI and vegetation parameters was investigated at Kendall for all measurement dates using aircraft-based measurements of surface reflectance (except DOY 252 when the red and NIR reflectance data were not available due to a loose connection on the airborne radiometer). There was a strong, linear correlation between SAVI and both percent vegetation cover and vegetation biomass (Figure 6a). Based on these limited results at Kendall, it appeared that the SAVI was capable of monitoring the temporal changes in vegetation cover and biomass at a single site.

The SAVI was less successful in discriminating spatial differences in vegetation parameters (Figure 6b). For the two dates on which vegetation cover was measured at the eight METFLUX sites (DOYs 221 and 247), the correlation between SAVI and percent vegetation cover was positive but

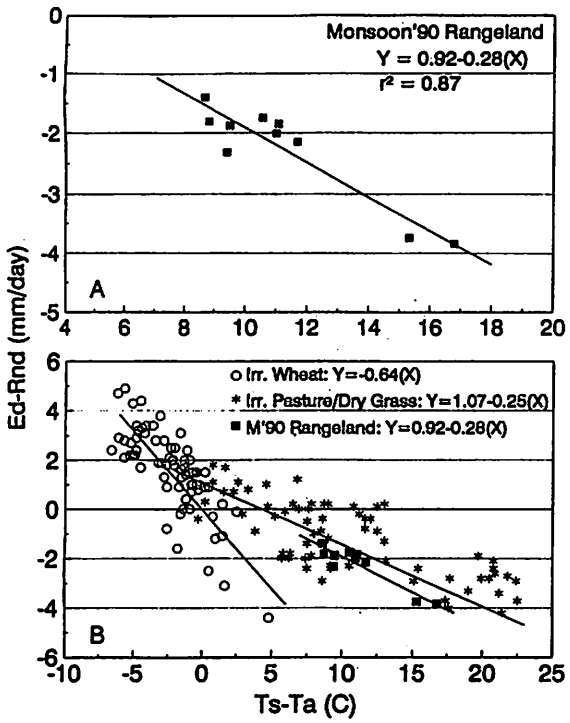

Figure 9. (a) Relation between daily surface evaporation rate (E_d) minus daily net radiation (R_{nd}) and surface-air temperature differences ($T_s - T_a$) at WGEW for the two METFLUX sites on DOY 156 and eight METFLUX sites on DOY 209. (b) Comparison of the rangeland data illustrated in Figure 9a with similar measurements of irrigated wheat published by *Jackson et al.* [1977] and irrigated pasture and dryland shortgrass published by *Seguin and Itier* [1983].

T_a made by *Seguin and Itier* [1983] for irrigated pasture and dryland shortgrass produced a slope and intercept quite similar to that for the Monsoon '90 rangeland data (Figure 9b). As a follow-up to the work of *Seguin and Itier* [1983], data from several "rangeland" experiments were combined and analyzed (see references listed in Table 4 for experimental details). Though the data trends looked similar, analysis of variance (ANOVA) indicated that the slopes of each data set were significantly different from one another ($F = 35.06$, degrees of freedom equaled 5.83, $p < 0.001$). Thus the hypothesis that the B value was independent of location for rangeland sites was rejected. Consequently, it was not appropriate to combine all the data sets in an attempt to derive a "universal" slope and intercept for these similar sites. However, it does appear that the slope derived by *Seguin and Itier* [1983] for medium-rough surfaces with unstable conditions (equation (8)) corresponds well with these measurements. This is encouraging, considering that these data sets were acquired at different sites with different roughness and thermodynamic properties, and the $T_s - T_a$ values were measured at different times of day (though always near midday). These spatial and temporal differences may account for some of the scatter in the relation.

The results presented in Figures 9b and 10 support the opinion [*Seguin and Itier*, 1983] that the relation between ($T_s - T_a$) and ($E_d - R_{nd}$) for stable conditions is different than that for unstable conditions. Noting the difference between the slopes for irrigated agriculture and rangeland data, it also supports the theory that sufficiently accurate values of $E_d - R_{nd}$ can be obtained using (5) by stratifying targets into only two or three general categories [*Carlson and Buffum*, 1989]. In any case, results presented in Figure 10 imply good potential for developing a simple relation such as (8) that would be useful for estimating evaporation rates of rangelands.

Concluding Remarks

The results presented here are both discouraging and encouraging. For this sparsely vegetated rangeland site, relations were found between spectral data and hydrologic parameters such as vegetation cover, soil moisture, and

Table 4. Description of Biophysical Characteristics of the Data Sets Presented in Figures 9 and 10, With Associated References

Data Set	Location	Vegetation Type	Reference	z_0	Comment
1	Phoenix, Arizona	irrigated wheat	*Jackson et al.* [1977]	≈10 cm	a single growing season, winter 1975/1976
2a	Crau, France	irrigated pasture	*Seguin and Itier* [1983]	1 cm	Crau plain, SE France, ground-based measurements of T_s at regional scale
2b	Crau, France	dryland shortgrass	*Seguin and Itier* [1983]	2 mm	Crau plain, SE France, ground-based measurements of T_s at regional scale
3	WGEW Arizona (1990)	grass and shrubland	*Kustas et al.* [1991]	1–4 cm	eight METFLUX sites, dry and monsoon seasons, aircraft-based measurements of T_s
4	Owens Valley, California	grass and shrubland	*Moran et al.* [1992]	≈5–10 cm	two site (grass and shrubland), June 1986, aircraft-based measurements of T_s
5	WGEW, Arizona (1992)	grass	*Moran et al.* [1993]	1 cm	Kendall METFLUX site, April–November, ground-based measurements of T_s

Data sets 1–3 are illustrated in Figure 9b; data sets 2–5, the rangeland sites, are illustrated in Figure 10. WGEW denotes Walnut Gulch experimental watershed.

reflectance factors from atmospheric and view angle corrected SPOT-1 HRV data, *Remote Sens. Environ.*, *32*, 203–214, 1990.

Moran, M. S., R. D. Jackson, and R. J. Reginato, Evaluating evaporation from rangeland vegetation by use of airborne radiometry and ground-based meteorological data using the Penman equation, in Evapotranspiration Measurements of Native Vegetation, Owens Valley, California, June 1986, *U.S. Geol. Surv. Water Resour. Invest.*, *91-4159*, 71–80, 1992.

Moran, M. S., et al., Evaluating energy balance of semiarid rangeland from combined optical-microwave remote sensing, paper presented at Topical Symposium on Combined Optical-Microwave Earth and Atmosphere Sensing, Inst. of Electr. and Electron. Eng., Albuquerque, N. M., March 22–25, 1993.

Moran, M. S., W. P. Kustas, A. Vidal, D. I. Stannard, J. H. Blanford, and W. D. Nichols, Use of ground-based remotely sensed data for surface energy balance evaluation of a semiarid rangeland, *Water Resour. Res.*, this issue.

Perry, E. M., and M. S. Moran, An evaluation of atmospheric corrections of radiometric surface temperatures for a semiarid rangeland watershed, *Water Resour. Res.*, this issue.

Pinter, P. J., Jr., R. D. Jackson, S. B. Idso, and R. J. Reginato, Diurnal patterns of wheat spectral reflectances, *IEEE Trans. Geosci. Remote Sens.*, *GE-21*(2), 156–163, 1983.

Ranson, K. J., and C. S. T. Daughtry, Scene shadow effects on multispectral response, *IEEE Trans. Geosci. Remote Sens.*, *GE-25*(4), 502–509, 1987.

Rosema, A., Comparison of Meteosat-based rainfall and evapotranspiration mapping in the Sahel region, *Int. J. Remote Sens.*, *11*, 2299–2309, 1990.

Schmugge, T., T. J. Jackson, W. P. Kustas, R. Roberts, R. Parry, D. Goodrich, S. A. Amer, and M. A. Weltz, Push broom microwave radiometer observations of surface soil moisture in Monsoon '90, *Water Resour. Res.*, this issue.

Seguin, B., and B. Itier, Using midday surface temperature to estimate daily evaporation from satellite thermal IR data, *Int. J. Remote Sens.*, *4*, 371–383, 1983.

Sellers, P. J., Y. Mintz, C. Sud, and A. Dalcher, A simple biosphere model (SiB) for use within general circulation models, *J. Atmos. Sci.*, *43*, 505–531, 1986.

Shuttleworth, W. J., and J. S. Wallace, Evaporation from sparse crops—An energy combination theory, *Q. J. R. Meteorol. Soc.*, *111*, 839–855, 1985.

Simanton, J. R., M. A. Weltz, and H. D. Larsen, Rangeland experiments to parameterize the water erosion prediction project model: Vegetation canopy cover effects, *J. Range Manage.*, *44*, 276–282, 1991.

Singh, S. M., and A. P. Cracknell, Effect of shadows cast by vertical protrusions on AVHRR data, *Int. J. Remote Sens.*, *6*, 1767–1771, 1985.

Slater, P. N., S. F. Biggar, R. G. Holm, R. D. Jackson, Y. Mao, M. S. Moran, J. M. Palmer, and B. Yuan, Reflectance- and radiance-based methods for the in-flight absolute calibration of multispectral sensors, *Remote Sens. Environ.*, *22*, 11–37, 1987.

Soil Conservation Service, National Range Handbook, *Rep. NRH-1*, U.S. Dep. of Agric., Washington, D. C., July 1976.

Stannard, D. I., J. H. Blanford, W. P. Kustas, W. D. Nichols, S. A. Amer, T. J. Schmugge, and M. A. Weltz, Interpretation of surface flux measurements in heterogeneous terrain during the Monsoon '90 experiment, *Water Resour. Res.*, this issue.

Tillman, J. E., The indirect determination of stability, heat and momentum fluxes in the atmospheric boundary layer from simple scalar variables during dry unstable conditions, *Appl. Meteorol.*, *11*, 783–792, 1972.

Tucker, C. J., Red and photographic infrared linear effects in remote sensing, *Remote Sens. Environ.*, *8*, 127–150, 1979.

S. A. Amer, Department of Hydrology and Water Resources, University of Arizona, Tucson, AZ 85721.

T. R. Clarke and M. S. Moran, USDA Agricultural Research Service, U.S. Water Conservation Laboratory, 4331 East Broadway, Phoenix, AZ 85040.

W. P. Kustas, USDA Agricultural Research Service, Hydrology Laboratory, BARC-East, Beltsville, MD 20705.

M. Weltz, USDA Agricultural Research Service, Southwest Watershed Research Center, 2000 East Allen Road, Tucson, AZ 85719.

(Received August 13, 1992; revised April 21, 1993; accepted October 19, 1993.)